

Short-Cavity Integrated VECSELs: A Fabrication Approach

Wolfgang Schwarz

We outline the fabrication of an electrically pumped surface-emitting laser with a short vertical extended cavity (VECSEL) for sensing applications. The emission wavelength is detuned by introducing microparticles into the cavity via a microfluidic channel. Multiple longitudinal modes can fit inside the resonator. A reproducible detuning of the extended cavity demands a longitudinal mode spacing of at least a few nanometers. The related resonator length of $80\ \mu\text{m}$ therefore requires a tailored fabrication and mounting procedure.

1. Introduction

For gas sensing, locking a laser to an atomic transition line, or detecting biological samples, a single-pass scheme is most commonly used [1–3]. Here the optical field is absorbed or scattered during a single encounter with the sample under test.

The cross-section can be enhanced if the sample is part of an optical resonator, as demonstrated for THz spectroscopy [4] and for optically pumped VECSELs [5]. When the sample is introduced into the standing-wave pattern inside the extended cavity, it affects the laser mode and changes of the beam shape as well as of the emission wavelength are induced. The detection of the beam shape can be realized with an image sensor. Image processing has to be done to extract the modal pattern. Signal processing algorithms like multidimensional fast Fourier transform (FFT) have a $O(N\log N)$ complexity [6], with N being the number of image points. In a typical image, N can exceed 10^5 . Unlike the beam shape, the spectrum can be optically analyzed by a grating in a parallel fashion. The resulting signal can be captured by a single line of a charge-coupled device (CCD) with $N \approx 10^3$. Evaluation is thus much faster, which is a favorable advantage in high-throughput applications with frame rates in excess of 1 kHz.

2. Fabrication Steps

The presented device consists of three functional elements, as shown in Fig. 1: (i) the vertical-cavity surface-emitting laser (VCSEL), interfaced electrically and thermally by a structured heat sink, (ii) the curved surface of the external mirror which is coated with a highly reflective coating, and (iii) a microfluidic channel carrying a suspension of the samples to be analyzed. This section describes the fabrication of the elements in detail. The requirement of a $80\ \mu\text{m}$ short extended resonator including a microfluidic channel puts tight constraints onto the fabrication procedure: Bond wires are too thick to interface the device electrically. Thus flip-chip mounting is the only approach which allows to shrink the cavity to the necessary length.

2.1 VCSEL and heat sink

The VCSEL was grown on silicon-doped GaAs by molecular beam epitaxy. The structure consists (in growth direction) of an AlAs etch stop layer, a distributed Bragg reflector (DBR) for the output coupler, an undoped barrier region of GaAs for the inner cavity embedding three quantum wells with a thickness of 8 nm each, and a highly reflecting DBR with a phase matching layer. Modulation doping with silicon and carbon is employed to achieve low optical and electrical losses in the n-doped output coupler and the p-doped reflector. The Al content in the AlGaAs DBRs is varied between 0.2 and 0.9 for sufficient index contrast. The p-mirror includes a thin AlAs layer for oxide confinement. After substrate removal, any Al containing surfaces are prone to corrosion. Therefore the phase matching layer is terminated by a GaAs layer which is sufficiently chemically stable. However, this layer absorbs light with wavelengths shorter than 870 nm by a fraction of approximately 10^{-3} nm^{-1} , which is too much for being part of an optical resonator with an enhanced field at this layer. For this reason, the layer structure was tuned for laser emission at 895 nm, which requires $\text{In}_{0.06}\text{Ga}_{0.94}\text{As}$ quantum wells. After wet etching of the p-mesas, the underetched microresist present on top of the mesas was not stripped, but used as a lift-off mask for the subsequent evaporation of the Ge/Au/Ni/Au n-contact. The AlAs layer in the p-doped DBR exposed by mesa etching was selectively oxidized to diameters ranging from 6 μm to 20 μm in water vapor at 646 K. The p-contact metals Ti/Pt/Au were evaporated in a lift-off process. Gold electroplating was done on the n-contact to grow vias with the same height as the mesas, and the surface between the mesas and vias was passivated with Durimide[®]. The complete wafer surface was metalized with a diffusion barrier of Ta/Au to suppress penetration of the solder metal into the vias and mesas. About 500 nm thick Au was plated onto the mesas and vias and the exposed diffusion barrier was dry etched with argon and tetrafluoromethane. The wafer substrate was thinned to 170 μm thickness and diced into $1.5 \times 1.5 \text{ mm}^2$ pieces. The heat sinks were structured on floating zone (FZ) high-purity silicon with a specific resistivity $> 10^4 \Omega \cdot \text{cm}$. A thin layer of Al_2O_3 was sputtered on the wafers, acting both as passivation and as etch stop layer in the following dry etching steps. A thin Ta/Au layer was sputtered

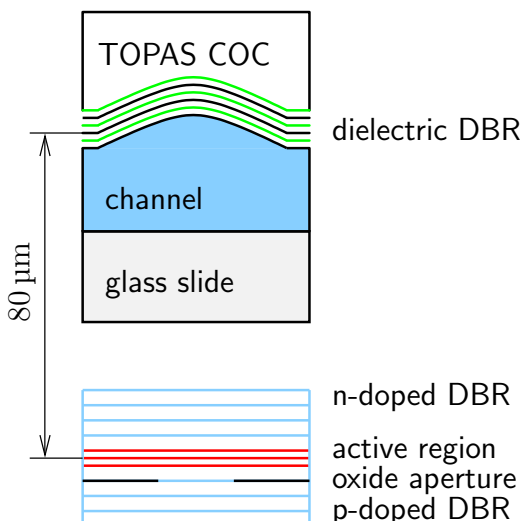


Fig. 1: Schematic drawing of the resonator structure. It comprises the VCSEL at the bottom, the microfluidic channel, and the hot-embossed concave-shaped Topas[®] COC channel wall, which is coated with a dielectric Bragg reflector to form the resonator mirror. Electrical contacts and the heat sink are omitted.

on the wafer surface as a seed layer for plating. Tracks of 2 μm thick Au were plated, which act as etch mask for dry etching of the exposed seed layer. The wafer surface was planarized with Durimide[®], leaving apertures for the solder bumps and the bondpads. A diffusion barrier of Ta/Au was sputtered on the wafer surface and 500 nm of Au were plated on the apertures for the bumps. Again the second diffusion barrier was dry etched. The micromachining was finished by evaporation of 4 μm In in a lift-off process for the solder bumps and dicing of $1.8 \times 12.3 \text{ mm}^2$ pieces. The VCSEL chips and the heat sinks were flip-chip soldered in a formic acid atmosphere at 473 K. The solder gap between VCSEL chip and the heat sink was filled with Crystalbond[™] to stabilize the chip during substrate removal. The substrate was spray etched in a $\text{NH}_4\text{OH} : \text{H}_2\text{O}_2$ solution down to the etch stop layer. The etch stop layer and the Crystalbond[™] were removed with diluted hydrofluoric acid and an organic solvent, respectively. The remaining epitaxial layers of the laser are fragile and were mechanically fixed with an underfill (Loctite[™] 3593).

2.2 External mirror and microfluidic channel

The external mirror was hot-embossed into cyclo-olefin-copolymer Topas[®] COC 5013 at temperatures close to the glass transition temperature of 400 K. Topas[®] COC material was chosen for its low birefringence and high transparency. Contrary to polymethyl methacrylate (PMMA), its low water absorption prevents swelling in water, and it supports the deposition of stable dielectric mirrors with thicknesses up to a few micrometers, which is crucial for the present application. By reactive ion beam sputter deposition of oxides of aluminum and tantalum, mirror reflectivities in excess of 98 % have been realized on BK7 glass, as shown in Fig. 2. The radius of curvature of the embossed external mirror ranges from about 160 to 290 μm and allows stable resonator modes for beam waists of

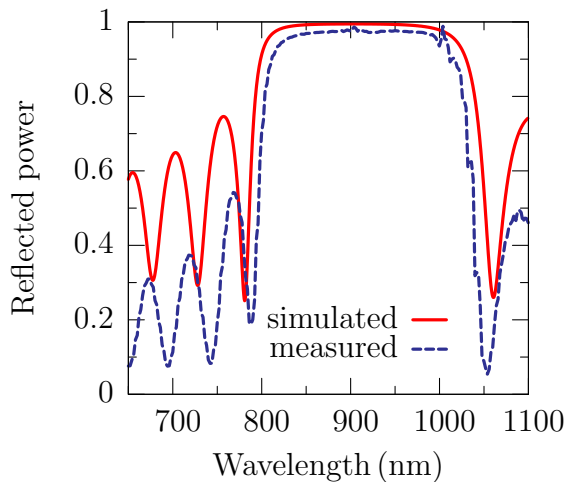


Fig. 2: Measured and simulated power reflectivity spectrum of a 9.5 pairs DBR coating on BK7 glass.

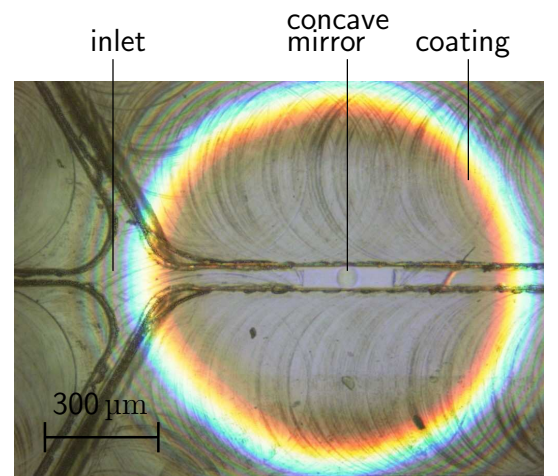


Fig. 3: Optical confocal microscope image of an embossed fluidic channel with an inlet for hydrodynamic focusing and a concave resonator mirror which is coated with a dielectric DBR.

8 and 10 μm . Figure 3 depicts the embossed channels. There is an inlet with one center channel for injection of the particles and two outer channels for a sheath fluid. If the flow rate of the sheath fluid is higher than in the center, the particles are confined to the center of the channel (hydrodynamic focusing [7]). The channel is wide enough to limit the clipping losses of the resonator. In the region of the resonator mirrors, the channel walls are coated with a dielectric DBR via a shadow mask. A 30 μm thin glass slide is fixed to the channel by compression bonding which closes the channel vertically. As a last step, the VCSEL is forward biased, actively aligned to the concave-shaped mirror for laser operation and fixed with a photocurable adhesive.

3. Conclusion

The fabrication of an integrated optical sensor based on an extended vertical resonator is demonstrated and details of the fabrication process are presented. Extensive characterization will follow in the near future.

We thank the Karlsruhe Institut für Technologie (KIT), Institut für Mikrostrukturtechnik for providing the microfluidic chips. This project is financed by the Baden-Württemberg Stiftung gGmbH.

References

- [1] A. Hangauer, A. Spitznas, J. Chen, R. Strzoda, H. Link, and M. Fleischer, “Laser spectroscopic oxygen sensor for real time combustion optimization”, *Procedia Chemistry*, vol. 1, no. 1, pp. 955–958, 2009.
- [2] S. Knappe, “MEMS Atomic Clocks”, Chap. 3.18 in *Comprehensive Microsystems*, Y. Gianchandani, O. Tabata, and H. Zappe (Eds.), pp. 571–612. Amsterdam: Elsevier, 2008.
- [3] P.K. Horan and L.L. Wheeless, Jr., “Quantitative single cell analysis and sorting”, *Science*, vol. 198, no. 4313, pp. 149–157, 1977.
- [4] R. Mendis, V. Astley, J. Liu, and D.M. Mittleman, “Terahertz microfluidic sensor based on a parallel-plate waveguide resonant cavity”, *Appl. Phys. Lett.*, vol. 95, no. 17, pp. 171113-1–3, 2009.
- [5] P.L. Gourley, “Biocavity laser for high-speed cell and tumour biology”, *J. Phys. D: Appl. Phys.*, vol. 36, no. 14, pp. 228–239, 2003.
- [6] M. Frigo and S.G. Johnson, “Design and implementation of FFTW3”, *Proc. IEEE*, vol. 93, no. 2, pp. 216–231, 2005.
- [7] M.L. Shuler, R. Aris, and H.M. Tsuchiya, “Hydrodynamic focusing and electronic cell-sizing techniques”, *Appl. Microbiol.*, vol. 24, no. 3, pp. 384–388, 1972.